Hybrid Nonlinear Model Predictive Control of a Cooling Water Network

J.H. Viljoen[a], C.J. Muller[a], I.K. Craig[a,*]

[a]*Department of Electrical, Electronic, and Computer Engineering, University of Pretoria, Pretoria, South Africa.*

Abstract

A Hybrid Nonlinear Model Predictive Control (HNMPC) strategy is developed for temperature control and power consumption minimisation of a cooling water network. The HNMPC uses a gradient descent optimisation algorithm for the continuous manipulated variables, and an enumerated tree traversal algorithm to control and optimise the Boolean manipulated variables. The HNMPC is subjected to disturbances similar to those experienced on a real plant, and its performance compared to a continuous Nonlinear Model Predictive Control (NMPC) and two base case scenarios. Power consumption is minimised, and process temperature disturbances are successfully rejected. Monetary benefits of the HNMPC control strategy are estimated.

Keywords: Nonlinear Model Predictive Control, Cooling Tower, Cooling Water Network, Optimisation, Gradient Descent, Hybrid Systems, Electricity Consumption Minimisation

1. Introduction

The benefits of applying Advanced Process Control (APC) to petrochemical plant utilities is becoming more apparent as such plants are coming under increasing pressure to lower their carbon footprints. Increasing attention is therefore being paid in the literature to the optimisation of utility systems through

*Corresponding author. Tel.: +27 12 420 2172.
Email addresses: henning@swissmail.org (J.H. Viljoen), nelismuller@gmail.com (C.J. Muller), ian.craig@up.ac.za (I.K. Craig)

advanced control and optimisation techniques (Muller et al., 2011; Ricker et al., 2012; Deng et al., 2015; Muller and Craig, 2015, 2016, 2017; Dzedzemane et al., 2018; Yin and Li, 2018).

In this paper, HNMPC techniques are applied to control and optimise an induced draft cooling water network. A nonlinear dynamic model that includes induced draft cooling towers with parallel heat exchangers, pumps and a cooling water network as developed in Viljoen et al. (2018) is used to design and test the performance of a NMPC and HNMPC controller.

Manipulated Variables (MVs) that are both continuous and discrete are used. Such systems are known as hybrid systems (Camacho et al., 2010) and can be cast in the form of a Mixed-Integer Nonlinear optimisation/Programming (MINLP) problem (Belotti et al., 2013). The nonlinear optimisation technique applied as part of the optimisation and control algorithm is gradient descent for the continuous MVs (Qian, 1999; Grüne and Pannek, 2017), and graph traversal for the Boolean MVs (Floudas, 1995).

Gradient descent, also known as steepest descent, is a first-order iterative optimisation algorithm well suited to solving NMPC problems (Nocedal and Wright, 2006). Being a deterministic gradient based optimisation technique, optimality and stability can be guaranteed under the correct conditions for this method (Boyd and Vandenberghe, 2004; Grüne and Pannek, 2017). The gradient descent optimiser has robust characteristics when the objection function hyperspace has less well conditioned surfaces (Goodfellow et al., 2016) and is shown to enable fast convergence.

Graph traversal is well suited to finding the optimal configuration of Boolean MVs that will determine the plant state in a particular process scenario (Floudas, 1995; Belotti et al., 2013). Given a particular plant trajectory and prediction horizon, the algorithm can consider the options available for the Boolean MVs and make an optimal selection per controller iteration to minimise the objective function (Camacho and Bordons, 2007).

Cooling water network control was previously described in Muller and Craig (2017) in which an economic hybrid nonlinear model predictive control of a

dual circuit induced draft cooling water system was developed. This paper differs from Muller and Craig (2017) in that the pump and cooling tower fan speeds are used as continuous MVs, the control algorithm is deterministic, and the cooling water network is different and modelled using a different modelling philosophy (Viljoen et al., 2018).

Three control strategies are simulated for disturbance rejection scenarios seen on a real plant - two base cases with constant MVs, a NMPC controller with only continuous MVs, and a HNMPC controller with continuous and Boolean MVs. The control strategies are simulated for four process scenarios - power consumption minimisation; plant load, ambient temperature, and ambient humidity disturbance rejection. Ambient humidity has been identified as one of the most important disturbance variables to include in the control and optimisation of cooling water systems (Castro et al., 2000), and is therefore also investigated here.

The monetary benefits achieved by the HNMPC controller are estimated by simulating the closed-loop system when exposed to actual ambient conditions. The controller minimises the power consumption while at the same time maintaining control of the temperatures of the hydrocarbon streams, which results in significant cost savings for the plant owner.

2. Cooling water network case study

2.1. Process description and operation

The plant that is being controlled and optimised in this paper is shown at a high level in Figure 1. The first principles dynamic model used in this paper for the plant and controllers, has recently been published in Viljoen et al. (2018).

The cooling capacity is supplied by 3 Cooling Towers (CTs) in parallel. Cooling Water Return (CWR) is sprayed into each cooling tower at the top of the tower. At the bottom of the towers, the cooling water falls into a common Cooling Tower Basin (CTB). Airflow through the cooling towers is induced by induction motor driven fans at the top of the cooling towers.

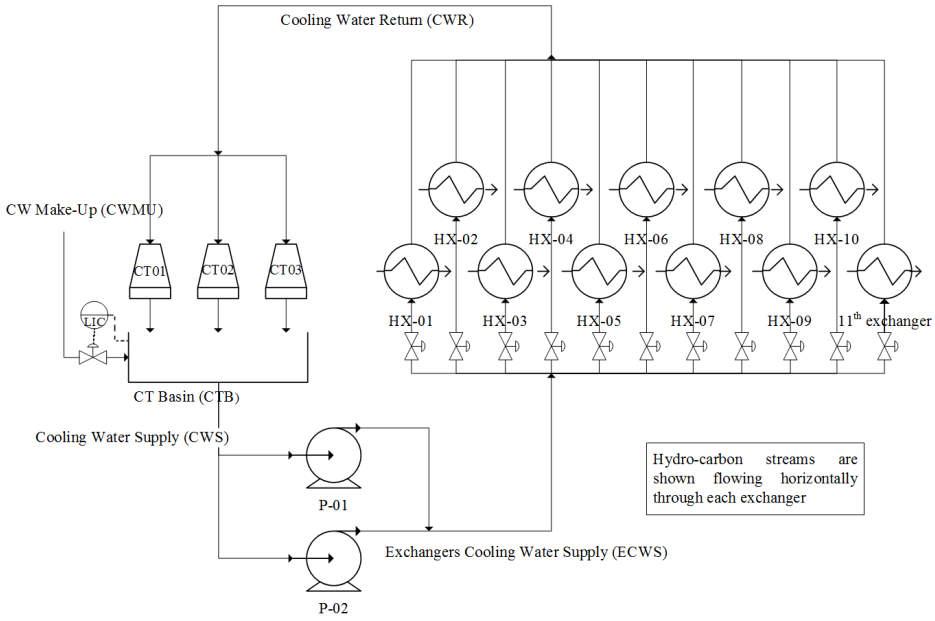

Figure 1: Overall layout of the Cooling Water Network.

Each tower is designed for a maximum flow rate of 8,700 m^3/h of cooling water, and heat duty of 101 MW. It is designed with a CWR temperature of 45 °C and a supply temperature of 35 °C in mind. Wet bulb temperature is designed to be 31 °C. Evaporative losses from the cooling tower are designed to be 1.83% of the total cooling tower flow.

The cooling tower fans are 9.1 m in diameter, and rotate at a design speed of 120.1 rpm. The design power consumption of each fan is 137 kW per fan.

Each pump is designed for an operating flow rate of 3850 m^3/h, and an operating discharge pressure of 5.3 barg. The design operating speed of each pump is 740 rpm, with a power consumption of 811 kW. However, in the actual plant it is running at a higher power operating point. The pumps need to supply the kinetic energy needed to move the cooling water through the entire cooling water network. In contrast the cooling tower fans are only moving air up the cooling tower. The water has much higher inertia and mass than the air,

therefore requiring much more electrical energy to power the pump motors.

133 parallel cooling water heat exchangers are fed with cooling water by the cooling towers and the pumps. Most of the heat exchangers are used to cool down process hydrocarbon streams. However, 73% of all the cooling water flows through the 10 biggest heat exchangers, and 27% flows through the remaining 123 smaller exchangers. As a simplification, the 123 smaller exchangers are lumped into a single heat exchanger in the model called the 11^{th} heat exchanger (Viljoen et al., 2018). After having passed through the 133 heat exchangers, the cooling water flows back to the cooling towers, completing the cooling water circuit.

The plant as described above is highly nonlinear, and interactive. The first principles dynamic model developed in Viljoen et al. (2018) for it consists of 80 differential state equations, 148 algebraic equations, 5 Boolean MV inputs, 16 continuous MV inputs, 16 Controlled Variables (CVs), 24 measured disturbances, and 86 model parameters.

The model is difficult to solve due to the stiff nature of the partial differential equations in the cooling tower models, the interactive nature of a closed-loop water system and the nonlinearity of the state and algebraic equations of each unit operation in the network.

The purpose of the cooling water network is to cool down various process hydrocarbon streams that form part of the petro-chemical facility and refinery adjacent to the cooling water plant. The cooling water Supply (CWS) streams flow into the larger facility, and returns back as CWR.

The plant as-is does not have automatic control controlling the hydrocarbon stream temperatures at the exit of each cooling water heat exchanger as shown in Figure 1. This results in potential significant fluctuation of the process temperatures as will be shown for the base case scenarios in this paper. Significant deviation from setpoint negatively effects the down stream processing equipment (e.g. reactors, distillation columns etc.) where a constant temperature for the hydrocarbon streams is what the equipment has been designed for.

The cooling water plant is subject to disturbances in the form of process

plant load changes, and ambient weather conditions changes. Typical 24 hour (midnight to midnight) ambient temperature and humidity that the cooling water plant is exposed to, are shown in Figure 2 and Figure 3.

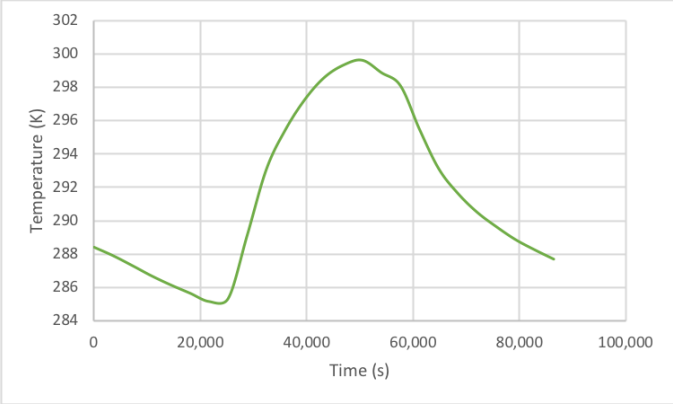

Figure 2: Typical 24 hour ambient temperature variation.

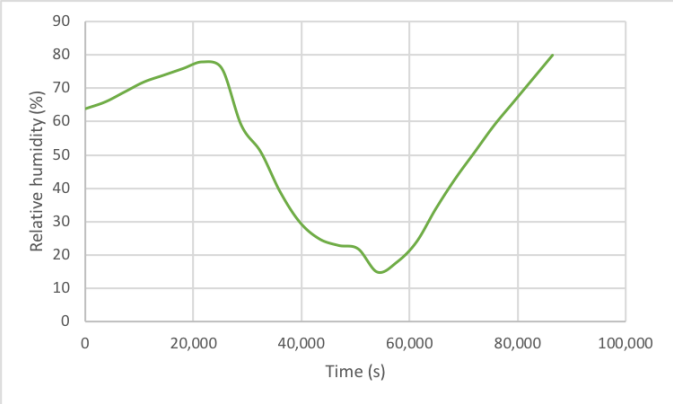

Figure 3: Typical 24 hour ambient relative humidity variation.

A plant disturbance that is fairly common in the facility modelled, is running the facility on 80% load during start-up or shut-down transients, or when maintenance or catalyst change-out is being carried out on one process train, or when the facility is being curtailed due to up-sets at the feedstock supplying company. This scenario is illustrated in Figure 4 that shows a simulated change

in the hydrocarbon total mass flow load. After 4 hours (14,400 seconds) the plant load is restored.

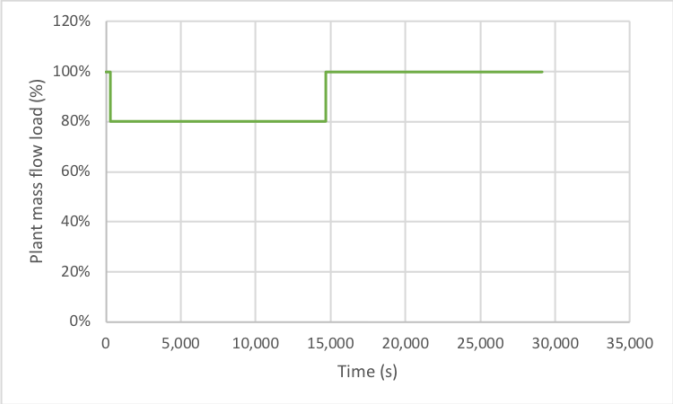

Figure 4: Plant hydrocarbon mass flow rates during plant load disturbance scenario.

2.2. Base case

The base case is the plant without any control and optimisation implemented. The only feedback control in the cooling water network is the PID level control of the cooling tower basin, where the level is controlled through make-up water.

In order to illustrate the power minimisation and then the temperature control capabilities of the control strategies developed in this paper separately, the base case is divided into two sub base cases: Base Case A, and Base Case B.

2.2.1. Base Case A

In Base Case A the fan and pump speeds are started at their design values, and the control strategies exploit the opportunity to decrease the speeds to optimal values while controlling temperature. The plant design speed for the cooling tower fans is 2 rps and for the pumps it is 12.33 rps (Viljoen et al., 2018). The cooling capacity generated at these speeds is only required during the warmest summer days when the ambient temperature and ambient humidity are at their highest. For the typical ambient conditions that the cooling water plant

is exposed to during evenings and most days the cooling capacity generated at these speeds is more than needed, resulting in more electric power consumption than is optimal for a given cooling requirement.

The uncontrolled plant in Base Case A experiences hydrocarbon temperature fluctuation due to the typical ambient temperature and humidity variations shown in Figure 2 and Figure 3. This is shown in Figure 5 for the temperature of the hydrocarbon outlet of HX-01.

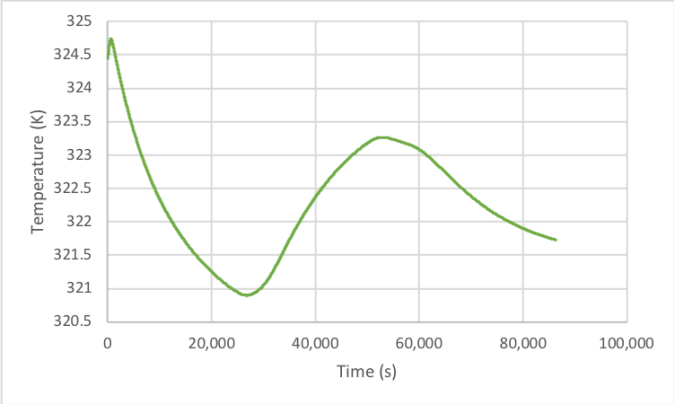

Figure 5: Base Case A: Uncontrolled HX-01 outlet temperature.

2.2.2. Base Case B

In Base Case B, the starting speeds of the fans and pumps are reduced to 1.2 rps and 9.75 rps respectively from that of Base Case A. This enables the control action to be less focused on power minimisation at typical ambient conditions, and more focused on temperature control.

For the uncontrolled plant in Base Case B, the hydrocarbon temperature fluctuates significantly from steady-state due to the process disturbances the cooling water plant is exposed to. This is shown in Figure 6 resulting from the plant load disturbance scenario as per Figure 4.

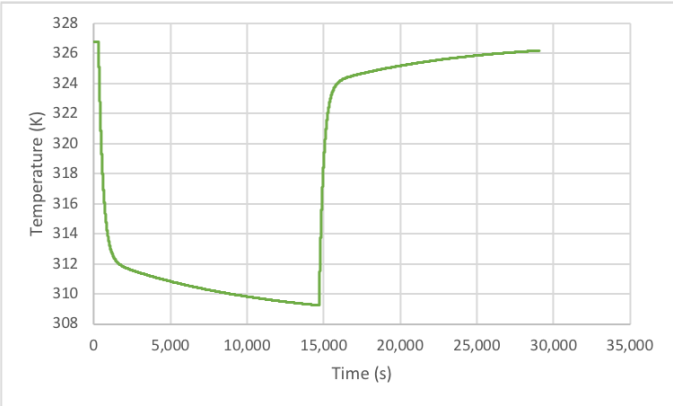

Figure 6: Base Case B: Uncontrolled HX-01 outlet temperature.

2.2.3. Monetary loss

Typical electricity rates for industries in the Arabian Gulf where the plant is located are USD 0.048 per kWh (Saudi Electricity Company, 2019). At this rate, and for the design fan and pump speeds as indicated above (Base Case A), the daily power consumption of the plant is 52,826 kWh, which translates into a daily power bill of USD 2,536.

2.3. Making the cooling water network amenable to Advanced Process Control

The uncontrolled plant does not have enough sensors and actuators for continuous NMPC nor HNMPC. Only the hydrocarbon process outlet streams of HX-04, HX-05, HX-06, HX-07 and HX-09 have temperature measurements (Viljoen et al., 2018). The other heat exchangers will need to have temperature measurements installed in order to enable APC strategies for the Cooling Water Network.

Saidur et al. (2012) and Al-Bassam and Alasseri (2013) show that energy consumption can be reduced when using Variable Speed Drives (VSDs). Continuous NMPC will require VSDs for the cooling tower fans and for the cooling water pumps. In addition, the fans and pumps will require some switch gear to enable on and off discrete switching of these equipment by the hybrid component of the HNMPC controller (see Section 3.1).

The hand valves that feed each cooling water heat exchanger with CWS, will need to be turned into control valves for the continuous NMPC controller to function. This will require different valve hardware as well positioners and actuators for each valve. The plant changes described above are assumed to be in place in what follows in order to demonstrate the benefits that can be achieved when using APC. Economic benefits assessment of APC technologies in general was surveyed in Bauer and Craig (2008).

3. Cooling water network control

In this section, two APC strategies, NMPC and HNMPC, are developed for the cooling water network model described in Section 2. The purpose of these controllers is to demonstrate the benefits that can be obtained over the two base cases described in Section 2.2.

3.1. Control objectives and framework

The control objectives are disturbance rejection for hydrocarbon process stream temperatures, power consumption minimisation for the cooling tower fans, and power consumption minimisation for the pumps.

The simulation results in Viljoen et al. (2018) show that a number of MVs can be used to control the process outlet temperatures of the heat exchangers. These MVs include the cooling tower fan speeds, the pump speed of the CWS pumps, and the valve openings of the cooling water flow to each exchanger. For control strategies in this paper, the hand valves upstream of each heat exchanger are modelled as equal percentage control valves.

The CVs for the system are the hydrocarbon process stream temperatures at the outlet of each heat exchanger (T_{HX_i}), the power consumption in each cooling tower fan motor (P_{f_i}), and the power consumption in each pump motor (P_{p_i}).

Three control strategies are used. The MVs applied depend on each control strategy:

1. Base case: No part of the plant is actuated, and the MVs are kept constant (see Section 2.2).
2. Continuous NMPC: The continuous MVs are included in an NMPC controller. In this scenario, the 11 hand-valves upstream of the CW side of each heat exchanger, are exchanged for positioner controlled control valves and included as continuous MVs in the controller (V_{OP}). The 3 cooling tower fan motors are assumed fitted with VSDs enabling the fan speeds (n) to be continuous MVs in the controller. The 2 cooling water pump motors are assumed fitted with VSDs enabling the pump speeds (ω) to become continuous MVs.
3. HNMPC: The 3 cooling tower fans on/off states, and 2 pump motor on/off states, are included as Boolean MVs in addition to the continuous MVs of control strategy 2.

The measured Disturbances Variables (DVs) of the system studied in this paper, are the ambient temperature and humidity, as well as the hydrocarbon mass flow rates and hydrocarbon input temperatures to the heat exchangers.

The capabilities of the NMPC and HNMPC controllers will be compared using the following process scenarios:

1. Power consumption minimisation.
2. Plant load disturbance rejection.
3. Ambient temperature disturbance rejection.
4. Ambient humidity disturbance rejection.

The industrial cooling water network on which this work is based is not currently automated. This paper shows what can be achieved if the temperatures and power consumption are controlled. The MVs (control valves, fan speeds and pump speeds) do have explicit operating ranges on the real plant and therefore the MV constraints are included in the control problem and designed controllers. Engineering unit CV ranges are defined as an order of magnitude of simulated range without explicit limits being available in order to be able to do normal-

isation of engineering units. The limits of the continuous CVs and MVs in engineering units are as per Table 1.

Table 1: Continuous CV and MV ranges.

Parameter	**Min.**	**Max.**	**Units**
Heat exchanger temperatures (11 CVs)	0	400	Kelvin
Cooling tower fan power (3 CVs)	0	300 000	W
Pump power (2 CVs)	0	3 000 000	W
Cooling tower fan speed (1 MV)	0.1	2.5	rps
Pump speed (1 MV)	1	14	rps
CW control valves (11 MVs)	0	1	fraction

3.2. NMPC

Linear Model Predictive Control (LMPC) has become the most popular multivariable control strategy in the process industries (Wang, 2009). A LMPC formulation can integrate optimal control, stochastic control, control of processes with dead time, and multivariable control (Camacho and Bordons, 2007). LMPC techniques have been used in (Ma et al., 2008; Marques et al., 2009; Li et al., 2012; Bakosova and Oravec, 2014; Deng et al., 2015; Yin and Li, 2018) to control utility and cooling water systems. LMPC makes use of a linear model, and in cases where the plant exhibits highly nonlinear behaviour, the controller response will often not be acceptable (Camacho and Bordons, 2007), hence the need for NMPC. This problem is exacerbated if the process spends a lot of time away from the stable design operating point of the LMPC. First principles models are often used for NMPC internal models (Sridhar et al., 2016). Significant progress has been made in NMPC research over the last few years (Allgower and Zheng, 2000; Findeisen et al., 2007; Negrete and D-Amato, 2013; Mayne, 2014; Biegler et al., 2015; Grüne and Pannek, 2017).

Deterministic NMPC methods are normally divided into two classes in the literature: Line search methods and trust region methods (Fletcher, 1987; Boyd

and Vandenberghe, 2004; Nocedal and Wright, 2006; Grüne and Pannek, 2017).
The NMPC problem utilising gradient techniques can be defined as follows:

$$\begin{aligned} &\min_{\mathbf{u}(\cdot)} J_N\left(\mathbf{x}_0, \mathbf{u}\left(\cdot\right)\right) \\ &\text{with respect to } \mathbf{u}\left(\cdot\right) \in \mathbb{U}^N\left(\mathbf{x}_0\right) \\ &\text{subject to } h\left(\mathbf{u}\right) \geq 0, \end{aligned} \tag{1}$$

where $J_N\left(\mathbf{x}_0, \mathbf{u}\left(\cdot\right)\right)$ is the objective function, $\mathbf{u}\left(\cdot\right)$ is a sequence of real valued vectors of the MVs, $\mathbb{U}^N\left(\mathbf{x}_0\right)$ is the set of admissible control sequences, $\mathbf{x}_0$ is the system state vector at initialisation, and $h\left(\mathbf{u}\right)$ is the inequality constraint function (Mayne, 2014; Grüne and Pannek, 2017). The control problem in this paper does not include equality constraints.

The objective function $J_N\left(\mathbf{x}_0, \mathbf{u}\left(\cdot\right)\right)$ is defined as

$$J_N\left(\mathbf{x}_0, \mathbf{u}\left(\cdot\right)\right) = \sum_{k=0}^{N-1} l\left(\mathbf{x}_{\mathbf{u}}\left(k, \mathbf{x}_0\right), \mathbf{u}_k\right) + V_f\left(\mathbf{x}_{\mathbf{u}}\left(N, \mathbf{x}_0\right)\right), \tag{2}$$

where l is the non-terminal cost, $\mathbf{x}_{\mathbf{u}}\left(k, \mathbf{x}_0\right)$ is the system state at sample time k as a function of $\mathbf{x}_0$ and the preceding MV control vector sequence $\mathbf{u}\left(\cdot\right)$, V_f is the terminal value of the objective function, and N is the prediction horizon Mayne (2014); Grüne and Pannek (2017).

In the NMPC literature, the control horizon normally refers to the number of control moves that are calculated in open-loop and sent to the plant, before feedback from the plant is fed into the controller again and the optimisation algorithm is run again (Grüne and Pannek, 2017). This definition is different from the definition for control horizon in LMPC (Camacho and Bordons, 2007). Shorter NMPC control horizons require shorter prediction horizons for the same stability guarantees (Grüne et al., 2012). In order to save on the required computational cost, shorter prediction horizons and control horizons are therefore preferred.

Gradient descent method, also called the steepest descent method (Nocedal and Wright, 2006), is a line search, first order, gradient based optimisation tech-

nique. Second order methods, also called Newtonian methods, include active set, and interior point methods (Fletcher, 1987; Boyd and Vandenberghe, 2004; Wright, 2004; Nocedal and Wright, 2006). Examples of Newtonian methods applied to NMPC problems are Lucia et al. (2013) and Biegler et al. (2015). The steepest descent gradient based algorithm is based on the Jacobian gradient vector of the system, and does not require the calculation of a Hessian matrix as required by Newtonian methods. Explicit computation of the Hessian matrix of second derivatives can be a computationally expensive process (Fletcher, 1987; Nocedal and Wright, 2006; DeHaan and Guay, 2007; Grüne and Pannek, 2017). Minimisation of the time the control algorithm will need to finish running, is an important goal to ensure practicality of the controller (see Section 4.7). Since the integration of the 80 state equations over the prediction horizon in the objective function is already computationally expensive, optimisation methods that do not require the Hessian are preferred and therefore used in this work.

For the steepest descent method, the objective function can be decreased by moving in the direction of the negative gradient of the system (Goodfellow et al., 2016) which is the direction in which the objective function decreases most rapidly (Nocedal and Wright, 2006):

$$\mathbf{u}_{k+1} = \mathbf{u}_k - \eta \nabla_{\mathbf{u}} J\left(\mathbf{u}_k\right) \tag{3}$$

where $\mathbf{u}_k$ is the MV vector for controller iteration step k, η is the learning rate and $\nabla_{\mathbf{u}} J\left(\mathbf{u}\right)$ is the Jacobian gradient vector of the objective function. The value of η can be set as a small constant through tuning, or various line search techniques can be used to set the value (Iusem, 2003; Boyd and Vandenberghe, 2004; Goodfellow et al., 2016).

Qian (1999) shows how the steepest descent algorithm can be made to converge faster and more robustly by adding an exponentially decaying (Sutskever et al., 2013) momentum term to the iterative equations. The convergence of the gradient iterations are accelerated by accounting for the history of iterations

when computing the ones to come (Ghadimi et al., 2015).

$$\begin{aligned} \Delta \mathbf{u}_{k+1} &= \gamma \Delta \mathbf{u}_k + \eta \nabla_{\mathbf{u}} J\left(\mathbf{u}_k\right) \\ \mathbf{u}_{k+1} &= \mathbf{u}_k - \Delta \mathbf{u}_{k+1} \end{aligned} \tag{4}$$

where γ is the exponential decay fraction of the previous step for the momentum term. During each iteration of the control algorithm, the MVs are adjusted by the term calculated as per (4). This momentum gradient descent algorithm is also called Polyak's heavy ball algorithm in the literature (Polyak, 1964). Gradient descent is known to start the optimisation quickly (Bryson, 1975), and momentum can considerably accelerate convergence to a local minimum (Polyak, 1964; Sutskever et al., 2013).

For the steepest descent algorithm, constraints can be managed through the projected gradient method where the optimisation variables are projected onto the allowed hyperspace at all times usually through an orthogonal method (Iusem, 2003). For box constraints (constant, linear constraints) on the variables to be optimised, this method modifies (4) as follows (Calamai and More, 1987):

$$\mathbf{u}_{k+1} = \Pi\left(\mathbf{u}_k - \Delta \mathbf{u}_{k+1}\right) \tag{5}$$

where $\Pi_i\left(u_i\right)$ is the projection function for one element of the $\mathbf{u}$ vector and is defined as

$$\begin{aligned} \Pi_i\left(u_i\right) &= \min\left(h_i, \max\left(l_i, u_i\right)\right) \\ &= \begin{cases} h_i, & \text{if } u_i > h_i \\ u_i, & \text{if } l_i \leq u_i \leq h_i \\ l_i, & \text{if } u_i < l_i \end{cases} \end{aligned} \tag{6}$$

where l_i is the lower bound constraint on u_i, and h_i is the upper (higher) bound constraint on u_i (Calamai and More, 1987).

Under the right conditions and convexity gradient based NMPC techniques, including the steepest descent algorithm are guaranteed to converge to a global minimum (Fletcher, 1987; Iusem, 2003; Boyd and Vandenberghe, 2004; Grüne and Pannek, 2017).

In Abbas et al. (2017) first order gradient descent was used for trajectory tracking for obstacle avoidance of autonomous road vehicles using NMPC. In Conceicao et al. (2008) steepest descent without momentum, and the conjugate gradient methods were used to solve the NMPC problem for trajectory tracking of a four-wheeled omnidirectional mobile robot. In DeHaan and Guay (2007) the steepest descent method, as well as a second order method where the Hessian is approximated were used to analyse real-time NMPC theory. In Guerreiro et al. (2014) both the steepest descent algorithm, and a Newton based line search algorithm was used to control an autonomous surface craft.

For the plant controlled in this paper, Viljoen et al. (2018) indicates that each discrete mode of the plant model has a convex hyperspace for the continuous MVs. This is indicated by the shapes of the curves of the CV responses to equal sized steps in the MVs from steady-state in (Viljoen et al., 2018). This implies that gradient based NMPC techniques can be used to apply NMPC to the plant (Grüne and Pannek, 2017) using the plant model developed in Viljoen et al. (2018).

NMPC problems have been shown in (Grüne and Pannek, 2017) to have stable closed-loop control solutions for the continuous control problem type of this work. The first order gradient descent methods of steepest descent (3), and steepest descent with momentum (4), were applied to the NMPC problem. Both methods resulted in stable closed-loop control, but the steepest descent with momentum method had superior performance with significantly faster convergence of the most important CVs to their set points in each process scenario simulated (see Section 4 for detailed results). Empirical closed-loop tuning of the exponential decay momentum factor γ and learning rate η were performed.

The constraints on the MVs for the control problem (see Table 1) are constant, linear constraints ("box constraints"). Therefore the projected gradient

method, (5) and (6), is applicable for handling the constraints in the NMPC algorithm and was implemented.

Derivative calculation for NMPC applications can be done through numerical differentiation, analytical derivation, symbolic math engines or automatic differentiation (Giftthaler et al., 2018). Analytical and symbolic approaches are often intractable for complex systems (Giftthaler et al., 2018), like the plant controlled in this paper. Automatic differentiation exploits the fact that every computer program executes a sequence of elementary arithmetic operations and elementary functions. By applying the chain rule repeatedly to these operations derivatives can be computed automatically (Baydin et al., 2018). The derivatives can be computed accurately to working precision, requiring a small constant factor more arithmetic operations than the original program (Bartholomew-Biggs, 2000). Automatic differentiation techniques, also called algorithmic differentiation (Giftthaler et al., 2017), are often divided into forward accumulation of gradients using the chain rule techniques, or reverse accumulation techniques (Neidinger, 2010). Automatic differentiation can be implemented using source code transformation, or operator overloading (Bartholomew-Biggs, 2000; Baydin et al., 2018). Walther (2007) has specifically shown how automatic differentiation can be applied to solve the optimal control problem of systems that use Runge-Kutta techniques to solve their state space equations.

Numerical differentiation has less numerical accuracy and computation speed compared to automatic differentiation (Bartholomew-Biggs, 2000). However, it enables faster setup time due to the significant additional software dependencies of automatic differentiation (Baydin et al., 2018). Numerical differentiation also has a high degree of error safety (Giftthaler et al., 2018) and is often used for these reasons (Grüne and Pannek, 2017). Lucia et al. (2013) also used numerical derivatives for the Jacobian. For all gradient based numerical nonlinear optimisation algorithms used in experiments and implemented in this paper, the one-sided-difference approximation was used to calculate the derivatives of the Jacobian vectors and Hessian matrices. At a given point $\mathbf{u}$ for the objective

function J,

$$\frac{\partial J}{\partial u_i}(\mathbf{u}) \approx \frac{J(\mathbf{u} + \epsilon e_i) - J(\mathbf{u})}{\epsilon} \tag{7}$$

where ϵ is a small scalar and e_i is the i^{th} unit vector, i.e. the vector of which the elements are all 0 except for a 1 in the i^{th} position (Nocedal and Wright, 2006).

3.3. HNMPC

The control of nonlinear plant models where the MVs are partly Boolean and partly continuous variables, are part of a collection of problems solved through control algorithms using Mixed Integer Nonlinear Programming (MINLP) models (Floudas, 1995). Real plants have both time-driven and event-driven dynamics, and control systems for such plants should preferably be able to accommodate both types (Camacho and Bordons, 2007). MINLP problems combine the combinatorial difficulty of optimising over discrete variable sets with the challenges of handling constrained continuous nonlinear functions (Belotti et al., 2013). These problems are usually much more complicated and expensive to solve than the corresponding continuous problem on account of the discrete nature of the variables and the combinatorial number of feasible solutions which thus can exist (Fletcher, 1987). The structure of these problems take the form

$$\begin{aligned} \min_{\mathbf{u}_R, \mathbf{u}_I} \; & J(\mathbf{u}_R, \mathbf{u}_I) \\ \text{s.t. } & h(\mathbf{u}_R, \mathbf{u}_I) \geq 0 \\ & \mathbf{u}_R \in \mathbb{U}_R \subseteq \mathbb{R} \\ & \mathbf{u}_I \in \mathbb{U}_I \subseteq \mathbb{I} \end{aligned} \tag{8}$$

where $J(\mathbf{u}_R, \mathbf{u}_I)$ is the objective function, $h(\mathbf{u}_R, \mathbf{u}_I)$ is the inequality constraint function, $\mathbf{u}_R$ is a real valued vector, and $\mathbf{u}_I$ is an integer valued vector (Floudas, 1995). $\mathbb{U}_R$ is typically a real valued set within the constraint boundaries for each real valued manipulated variable in $\mathbf{u}_R$. $\mathbb{U}_I$ is typically an integer

valued set within the constraint boundaries for each integer valued manipulated variable in $\mathbf{u}_I$

Each permutation of the discrete state variables could define a different plant state. These different plant states, will each have different continuous dynamics as per the hybrid automata of each state (Camacho and Bordons, 2007). If the number of possible discrete states that the plant can be in is large, (8) can be an NP-hard combinatorial problem (Belotti et al., 2013).

Most solution methods for MINLP in the literature apply some form of tree search (Belotti et al., 2013). If the integer variables in the problem are Boolean, the resulting state tree is a binary tree with two branches for every node. The nodes at level m in such a tree correspond to each of the 2^m nonlinear optimisation problems that would have to be solved if each node was visited during a brute force overall solution algorithm (Camacho and Bordons, 2007).

Instead of solving all the possible objective function minimisation problems defined by each possible combination of Boolean variables, alternatively branch and bound methods can be used to solve the MINLP problem (Camacho and Bordons, 2007). In addition to branch and bound other algorithms are also found in the literature (Floudas, 1995).

Mayer et al. (2016) used a linear approach with hybrid branch and bound methods to control a building cooling system supply. Cacchiani and DoAmbrosio (2016) developed a branch and bound algorithm to solve a unit commitment problem of a generation company whose aim is to find the optimal scheduling of a multi-unit pump-storage hydro utility power station. Although this problem is not a control problem, it is a case of a nonlinear constrained MINLP. In Long et al. (2007) deterministic HNMPC with a tree based algorithm was used to control the pressure of two pressure vessels in series taking in air as the process input. Deterministic nonlinear optimisation methods using tree graphs, are shown to be able to guarantee global optimality (Long et al., 2007), and be able to perform direct optimisation.

For the plant controlled in this paper, the 3 cooling tower fans, and the 2 cooling water pumps can be turned into Boolean MVs if the motors of the

rotating equipment can be switched on and off by the HNMPC controller. Due to the induction motors driving the fans and pumps exceeding their steady-state current by 500 to 800 percent during start-up (Viljoen et al., 2018), a natural deadband is introduced into the controller if the power is included for minimisation in the objective function, in order to limit unnecessary switching of the equipment.

The steepest descent with momentum NMPC controller designed in Section 3.2 for the continuous MVs, was combined with a graph traversal approach to optimise the discrete states that the plant can be in. This design resulted in an HNMPC controller based on first order gradient descent with momentum for the continuous MVs, and a tree based MINLP Boolean MV controller for the Boolean MVs.

At least one of the two pumps needs to run at all times since with no pumps running no cooling water would circulate in the network. This results in the number of effective Boolean MVs dropping from 5 to 4. The possible states that the plant can be in from the perspective of the hybrid controller, is shown in the tree graph of Figure 7. The graph is shown as a tree where each level of the tree shows the permuted possible states of 1 of the 4 Boolean MVs. The leaves of the tree in the lowest row when traced up to the root node, represent all the 16 possible permutations of discrete states the controller can put the plant in. The 3 cooling tower fans can all be off as a discrete plant state, or can be switched on one by one. If one pump is chosen to always be on, and each cooling tower is assigned a fixed role in the permutations of cooling tower states, the number of effective discrete plant states to be optimised between can be limited to 8 states as per Table 2. The MINLP problem to be solved by the HNMPC controller (8) can be an NP-hard problem, therefore any consolidation of plant discrete states that can be done as per Figure 7 will increase the controller viability and reduce computational cost. The reduced number of effective states are shown as the red nodes in Figure 7.

The number of possible plant states to be optimised between, and for which the NLP problem has to be solved each time the controller is run, has been

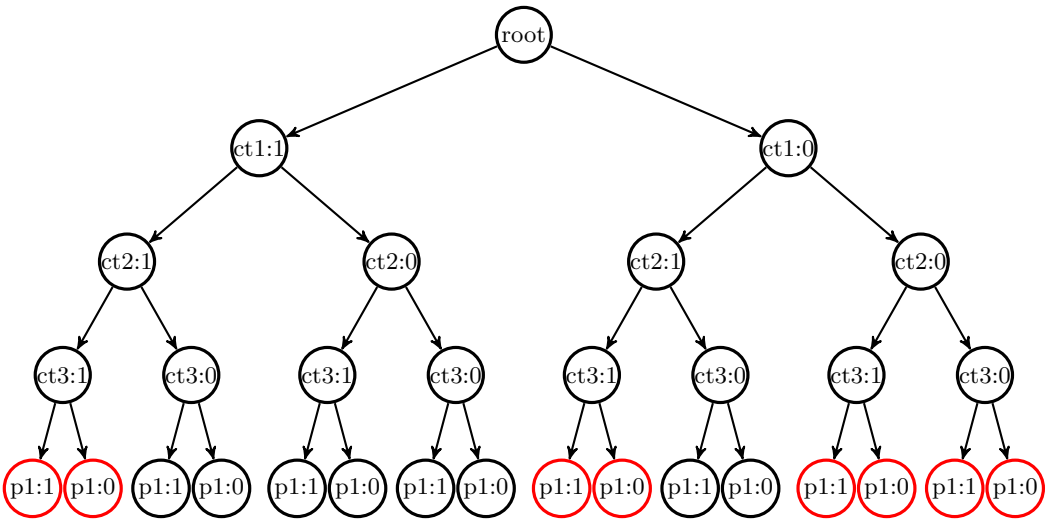

Figure 7: Hybrid controller state graph (Short hand: ctx:1 means cooling tower x fan is on, and ctx:0 means it is off. px:1 means pump x is on, and px:0 means it is off).

reduced through this consolidation so that all the essential states can be iterated over (Camacho and Bordons, 2007). If this is viable, then the need for a more complex and expensive algorithm like branch and bound (Belotti et al., 2013) can be averted. This approach was found to be viable for the HNMPC controller implemented.

During each iteration of the HNMPC controller, the objective function (9) is calculated for each plant state which is modelled as a red node on the plant state graph being traversed (Figure 7). The best node as per the objective function (9) is chosen, and the hybrid MVs switched accordingly given the current state of the continuous MVs. Then the gradient descent step for the continuous MVs is calculated and implemented with (4). After this, the iteration step is completed, and the algorithm will start again with traversing the tree nodes at the next controller iteration. This high-level algorithm is portrayed in pseudo code in Algorithm 1.

A logic block is inserted between the model and the NMPC controller to take

Algorithm 1 HNMPC controller algorithm

```
Initialise plant model.
Initialise Boolean MVs.
Initialise continuous MVs.
for the simulation period do
    Integrate plant model state equations one step.
    if controller waiting period complete according controller frequency then
        for all effective discrete plant states do
            Evaluate objective function for plant state
        end for
        Select Boolean MVs of plant state with highest objective function.
        Calculate continuous MV Jacobian gradient of objective function.
        Calculate the new continuous MV values with the gradient.
        Apply the projected gradient method for constraint handling.
        Implement gradient descent continuous MV step for the gradient.
    end if
end for
```

Table 2: Discrete plant states as determined by Boolean MVs.

State nr	CT 1	CT 2	CT 3	Pump 1
1	1	1	1	1
2	0	1	1	1
3	0	0	1	1
4	0	0	0	1
5	1	1	1	0
6	0	1	1	0
7	0	0	1	0
8	0	0	0	0

a single continuous MV from the NMPC controller for fan speed, and duplicate it across all 3 fans. The same is done for the 2 pumps. This approach simplifies the NMPC design. Individual motors can still be shut-down and started up by the Boolean MVs of the HNMPC controller independent from each other.

The objective function to be minimised by the HNMPC controller, is a weighted sum of the 3 classes of CVs in the controller (see Section 3.1):

$$J_N = \frac{1}{N}\sum_{i=1}^{N}\left(\sum_{j=1}^{11} Q_{T_{HX_j}}\left(T_{HX_j} - T_{SPHX_j}\right)^2 + \sum_{j=1}^{3} Q_{P_{fj}}\left(P_{f_j} - P_{SPf_j}\right)^2 + \sum_{j=1}^{2} Q_{P_{pj}}\left(P_{p_j} - P_{SPp_j}\right)^2\right) \tag{9}$$

where the set point targets (e.g. T_{SPHX_j} for the temperature CVs) are subtracted in each summation from the heat exchanger outlet process temperatures (T_{HX_j}), the fan power consumptions (P_{f_j}), and the pump power consumptions (P_{p_j}) (Rubio-Castro et al., 2013). $Q_{T_{HX_j}}$, $Q_{P_{fj}}$ and $Q_{P_{pj}}$ are the weights for the heat exchanger hydrocarbon stream outlet temperatures, and fan and pump power error terms. The objective function is calculated and summed over a Prediction Horizon (N) of 45 minutes simulation time, each time the HNMPC control algorithm executes. In order to minimise computational cost, shorter

prediction horizons and shorter NMPC control horizons are preferred for a certain level of stability (Grüne et al., 2012). Therefore, the NMPC control horizon is 1 control move for the prediction horizon of 45 minutes. With this design, feedback from the plant is obtained after each control move that the controller algorithm sends to the plant.

The frequency of the controller executing one iteration was set to 10 minutes simulation time. The numerical plant model is iterated every 200ms due to the stiff nature of the plant model differential equations (Viljoen et al., 2018). No terminal constraint (Grüne and Pannek, 2017) was added to the objective function.

For the continuous-only NMPC scenarios, the same objective function (9) is used, but the Boolean MVs are not available to the controller to manipulate.

The power variables are always minimised in the objective function by setting the set point target equal to zero, and tuning the weight of the relevant term in (9). The HNMPC controller will not allow the MVs to move outside their limits (6), whereas CVs can but are penalised more in the objective function the further away from the set point targets they move.

Empirical tuning of the controller tuning constants was performed through simulation runs of the closed-loop system for all scenarios and control strategies with the goal of achieving tight control but also stability. Other parameter values experimented with either compromised on tightness of control, or stability of the closed-loop response. The maximum step size allowed for the continuous MVs during one controller iteration, was limited to 10% of the engineering unit range of the MV. The purpose of this limitation is to prevent severe disturbances to the plant due to potentially very aggressive action of the controller. Tuning constants and optimisation algorithm parameters were used in the controller as per Table 3.

The same tuning values for all controller parameters was used for both the NMPC and HNMPC controllers. A high-level portrayal of the plant and designed control system indicating the various MV and CV signals between the plant equipment and NMPC/HNMPC controller is shown in Figure 8. The 11

Table 3: Tuning parameters of NMPC and HNMPC controllers.

Parameter	**Symbol**	**Value**	**Units**
Momentum decay	γ	0.0925	
Learning rate	η	0.0625	
Objective weight HX temp.	$Q_{T_{HXj}}$	1	
Objective weight Fan power	$Q_{P_{fj}}$	0.00001	
Objective weight Pump power	$Q_{P_{pj}}$	0.0001	
Controller prediction horizon	N	45	Minutes
Controller running interval		10	Minutes
Controller NMPC control horizon		1	Control move
Maximum continuous MV change per iteration		10	% of EU range

parallel heat exchangers and 11 control valves are shown as 1 exchanger and valve to save space on the drawing.

The HNMPC controller is implemented in a C++ simulation platform (Stroustrup, 2013) that is able to control and optimise the plant model (Viljoen et al., 2018) with its stiff partial differential equations in real time.

4. Results and discussion

The NMPC and HNMPC controllers are simulated in closed-loop in the subsections that follow. The different scenarios are discussed separately with each control strategy simulated for each scenario. Subsequently the scenarios and strategies are compared and conclusions drawn.

All simulations are started with the plant running with an ambient temperature of 25 °C, and an ambient humidity of 50%. The power minimisation scenario is run over 24 hours of simulation time. The plant load disturbance, ambient temperature disturbance and ambient humidity disturbance rejection scenarios are started with 5 minutes of simulation time with the plant at steady-state before the disturbances are applied, followed by 8 simulation hours of disturbance rejection control. Only the fan and pump power is shown in figures

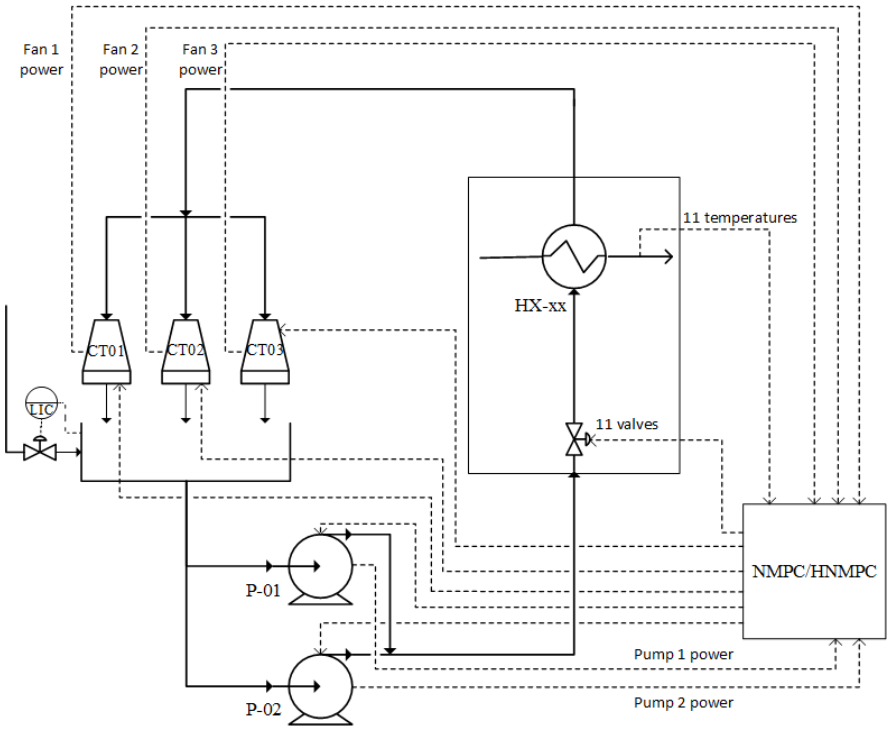

Figure 8: Overall control system design with NMPC/HNMPC, MV and CV signals.

and not the speed as well, in order to limit the number of figures in the paper. Since the speed and power variables are correlated, they will normally move in the same direction.

4.1. Power consumption minimisation

The design figures documented in Section 2.1 for the cooling tower fan speeds and cooling water pump speeds are higher than what is required for the ambient conditions the plant is typically exposed to. The continuous NMPC controller is able to exploit this opportunity when excess cooling capacity is being generated by ramping down the fan and pump speeds while maintaining the temperatures.

In this scenario the simulation is started with the fans and pumps running at their design speeds as per Base Case A in Section 2.2. The plant is exposed to a typical 24 hour ambient temperature and humidity cycle as per Figure 2

and Figure 3. The hydrocarbon stream temperatures at the outlet of HX-01 are shown in Figure 9 for the uncontrolled base case and when NMPC and HNMPC are used. The NMPC and HNMPC controllers are able to keep the temperature at set point, and have the same effect since fast discrete control action is not required due to the slowly varying disturbances.

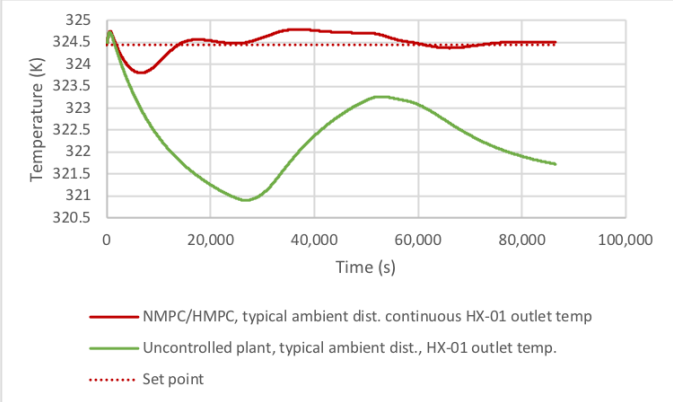

Figure 9: HX-01 outlet hydrocarbon temperature for power minimisation scenario.

The controllers decrease the fan speeds in order to minimise fan power as shown in Figure 10 while controlling temperature. Due to the cubed relationship between fan power and speed (Viljoen et al., 2018), a 40% reduction in speed results in a almost an 80% reduction in fan power.

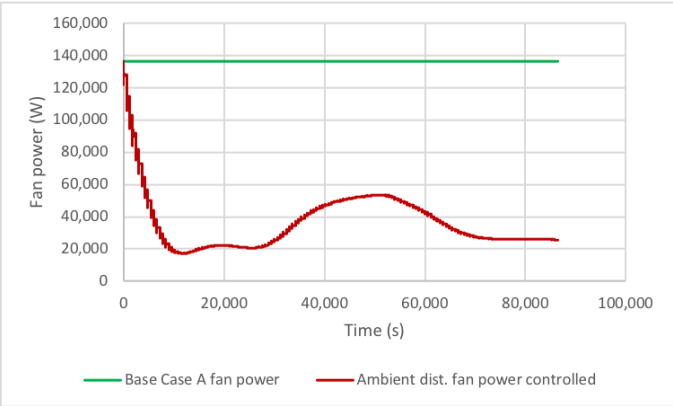

Figure 10: Cooling tower fan power for power minimisation scenario.

The pump speed is also reduced by the controller in order to minimise pump power as shown in Figure 11.

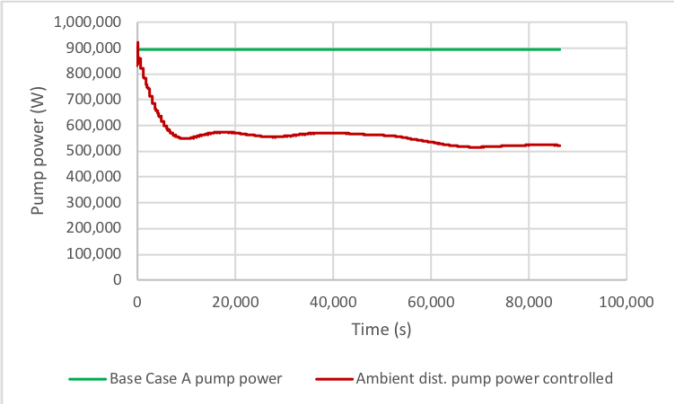

Figure 11: Cooling water pump power for power minimisation scenario.

Cooling water valve movement is negligible in this scenario since the ambient conditions change very slowly and adjusting cooling capacity in the circuit as a whole is needed. This cooling capacity adjustment is mainly done by the fan and pump speeds as opposed to the cooling water valves. As expected, the controllers focus on the fans and pumps as this is where the most power is consumed.

4.2. Plant load disturbance scenario

Base Case B as described in Section 2.2 is used here to compare the NMPC and HNMPC controllers to. The plant load disturbance applied is shown in Figure 4. The simulation is continued for another 4 hours after the plant loads have been restored to give the temperature time to settle.

The temperature disturbance rejection performance of the NMPC and HNMPC controllers are compared to Base Case B in Figure 12. The NMPC and HNMPC controllers optimise the cooling capability as much as possible, and limit the undershoot of the hydrocarbon temperatures. The HNMPC can contain the undershoot slightly better than the NMPC. When the plant load is restored, the controllers bring the temperature back to set point.

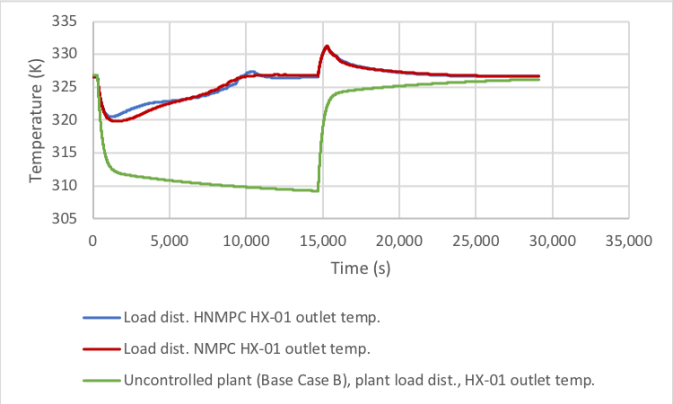

Figure 12: HX-01 outlet hydrocarbon temperature, with plant load disturbance.

The cooling tower fan power is minimised by the controller while still keeping the temperature under control (Figure 13). Under continuous control the controller is limited to moving the fan speed to not more than 10% of its range per control iteration. The fan speed is ramped down as fast as possible, and then ramped up again to limit temperature overshoot when the plant load is restored. This results in the fan power trend as in Figure 13. After the temperature is restored to set point, the fan speed is still ramped down somewhat to further minimise power consumption.

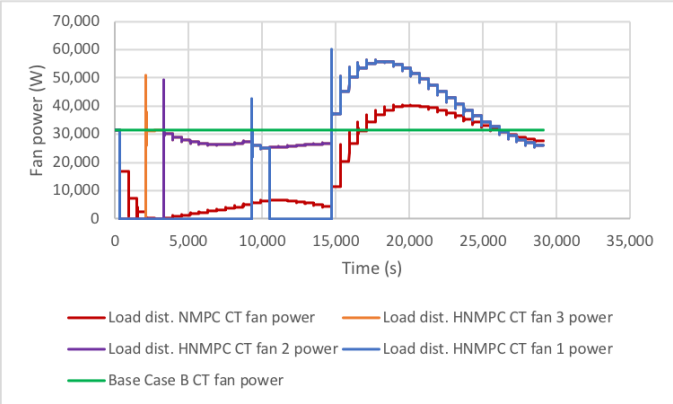

Figure 13: Cooling tower fan power with plant load disturbance.

Under HNMPC control, all 3 cooling tower fans are switched off by the controller as soon as the plant load drops thus minimising cooling capacity and saving power (Figure 13). Fan 2 is switched on again after around 2,500 seconds, followed by fan 3 at around 3,000 seconds. Fan 1 is switched on at 9,000 seconds, and switched off again at 11,000 seconds. When the plant load is restored, fan 1 is switched on again and all fans are ramped up and later down to limit temperature overshoot, and save power.

Under NMPC control the pump power is minimised (Figure 14) by turning the pump speeds down. When the plant load returns, the pump speeds are ramped up to prevent hydrocarbon temperature overshoot.

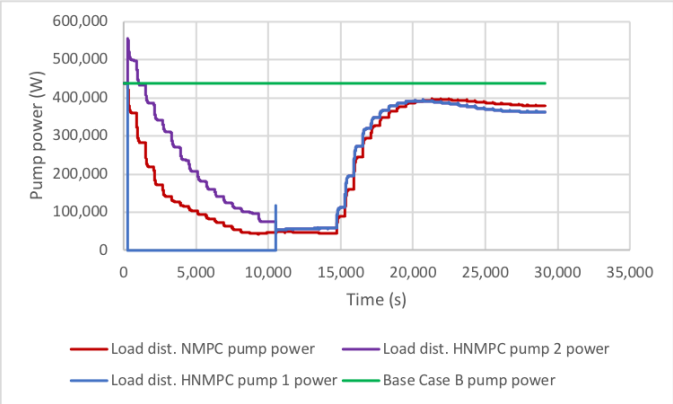

Figure 14: Cooling water pump power with plant load disturbance.

Under HNMPC control, pump 1 is shut down immediately when the plant load is reduced, thus minimising cooling capacity, as well as pump power (Figure 14). Pump 2 is kept on to supply cooling water to the plant but turned down to save power (Figure 14). The power consumption of pump 2 drops initially when pump 1 is switched on again, as less CW flows through it when pump 1 also starts pumping CW.

The CW valve movements during both NMPC and HNMPC are very similar, and are shown for valve 1 in Figure 15. The control valves move significantly in the plant load disturbance scenario since the effect of this disturbance has a

considerable effect on the temperature CVs with faster dynamics. This is due to the disturbance not being in the ambient conditions but very close to the CVs in the plant, thus effecting the CVs faster.

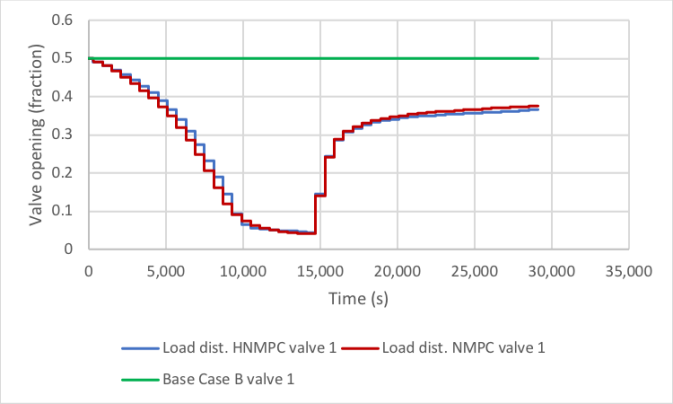

Figure 15: Cooling water valve 1 movement under continuous control with plant load disturbance.

4.3. Ambient temperature disturbance scenario

Changes in ambient conditions can have a large effect on the cooling tower performance. The ambient temperature changes in this scenario are made more rapidly than what would occur naturally. The performance of the controllers is compared to that of Base Case B as described in Section 2.2.2.

The NMPC and HNMPC controllers are required to maintain the hydrocarbon heat exchanger outlet temperatures at set point, and in addition to consume as little power as possible. The ambient temperature was first stepped down from a starting value of 25 °C to 5 °C and kept there for 4 hours to allow the controller to act and the variables to settle, then the temperature was stepped back to 25 °C for another 4 hour period (see Figure 16).

Both the NMPC and HNMPC restrict the drop in hydrocarbon outlet temperature and limit the overshoot above set point when the ambient temperature is restored (see Figure 17). The NMPC performs well, but the HNMPC performs significantly better in this scenario.

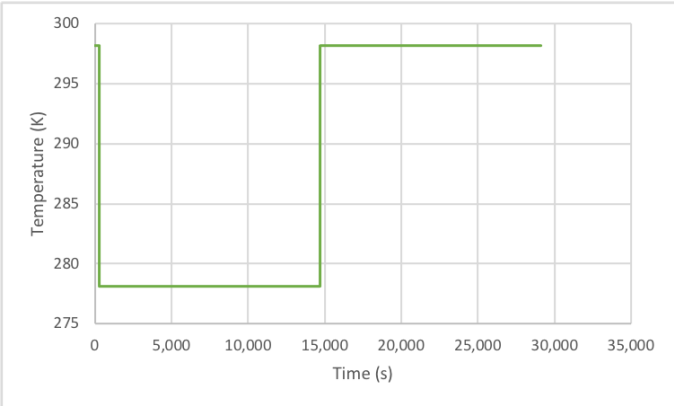

Figure 16: Ambient temperature during ambient temperature disturbance scenario.

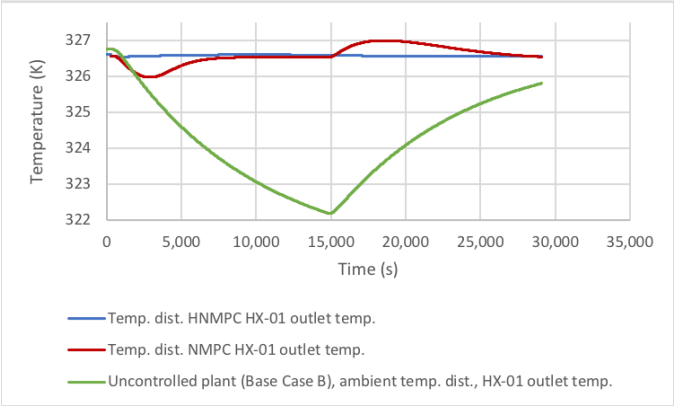

Figure 17: HX-01 outlet temperature during ambient temperature disturbance scenario.

The NMPC controller keeps reducing the CT fan speeds and power consumption (Figure 18) in order to minimise cooling when the ambient temperature drops. The HNMPC controller does not change the fan speeds for CTs 2 and 3. It does however shut down the CT 1 fan when the ambient temperature drops, and starts it up again when the ambient temperature increases as shown in Figure 18. In this way the HNMPC controller balances the demand for power minimisation and temperature control.

The CT fans have more of an influence on the hydrocarbon temperature than the speed of the pumps. The HNMPC controller therefore uses the pump

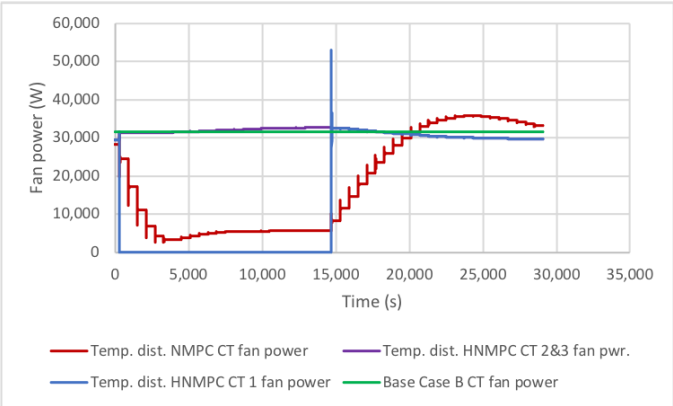

Figure 18: CT fan power during ambient temperature disturbance scenario.

speed MVs to mainly reduce the power consumption (Figure 19) in the circuit. It can afford to only make small changes to the pump speeds as it has shut down a CT fan (Figure 18) in order to reject the ambient temperature disturbance. The NMPC controller does not have this luxury, and therefore its pump speed movements are more pronounced, resulting in the pump power trend as in Figure 19.

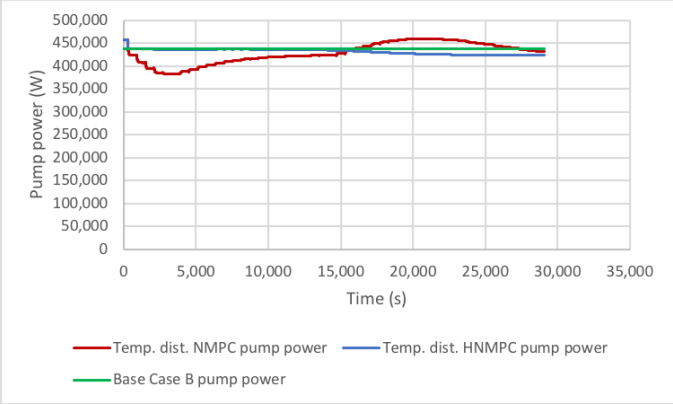

Figure 19: CW pumps power during ambient temperature disturbance scenario.

The control valve movements have less of an influence on the hydrocarbon temperature than the CT fans, and also a smaller influence on power consump-

tion than the CW pumps. The HNMPC controller does not need to change the valve opening much as it has shut down a CT fan (Figure 18) in order to reject the ambient temperature disturbance. The valve opening movements resulting from the NMPC controller are more pronounced as for the pump speeds (Figure 20).

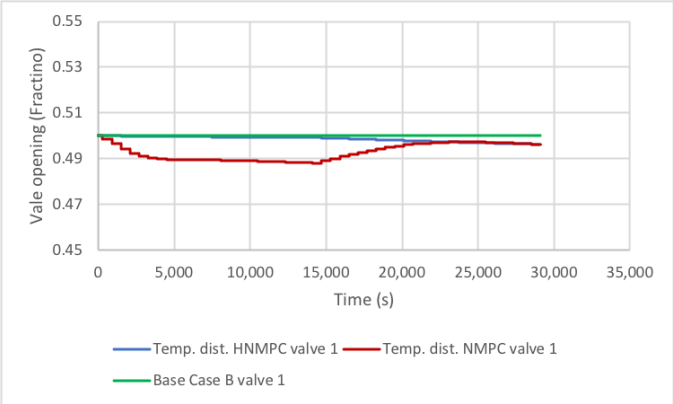

Figure 20: CW valve 1 movement during ambient temperature disturbance scenario.

4.4. Ambient humidity disturbance scenario

The ambient humidity changes are made more rapidly than what would occur naturally. The performance of the controllers is compared to that of Base Case B as described in Section 2.2. The relative humidity was first stepped down from a starting value of 50% to 0% and kept there for 4 hours to allow the controller to act and the variables to settle, then the humidity was stepped back to 50% for another 4 hours (see Figure 21).

Both controllers contain the hydrocarbon outlet temperature well compared to the uncontrolled plant Base Case B response (Figure 22). The hybrid controller does slightly better since it has more degrees of freedom with the Boolean MVs also at its disposal (see Table 5).

Both controllers ramp down the CT fan speeds (Figure 23) in order to contain the drop in hydrocarbon temperature when the ambient humidity is stepped down. The HNMPC controller shuts down fan 1 for some time in order to

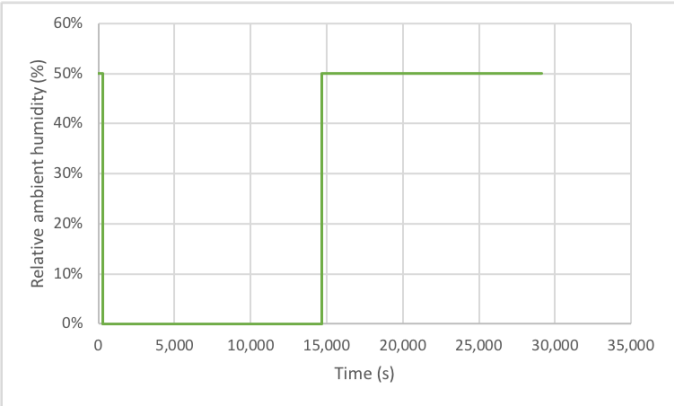

Figure 21: Ambient humidity steps to test humidity disturbance in the NMPC controller cases.

further minimise power (Figure 23) and assist in containing the temperature drop. The opposite occurs when the humidity is stepped back up.

The cooling water pumps are used mainly by the controllers to minimise power, and less to control temperature. That is the reason that the pump speeds are not moved much over the simulation time resulting in the pump power trends as in Figure 24.

Pump power consumption is further minimised over the life of the scenario (Figure 24), and when the temperature is under control again at the end of the scenario, the pump power consumption is slightly less than at the start of the scenario.

The cooling water valves are also moved to a much smaller degree by the controller during the ambient humidity steps. See Figure 25 for the trajectory of valve 1.

4.5. Simulation scenario and control strategy comparison

4.5.1. Base Case A

In Table 4, the power consumption and resulting electricity cost of the control strategies in the power consumption scenario are shown. Since no fast discrete action is required due to the slowly varying disturbances prevalent in

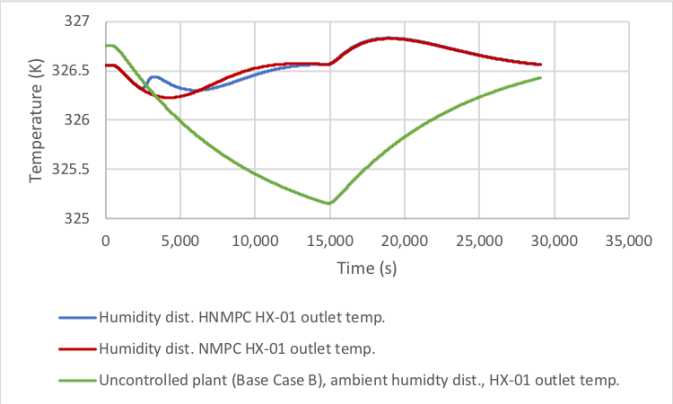

Figure 22: HX-01 outlet temperature during ambient humidity disturbance scenario.

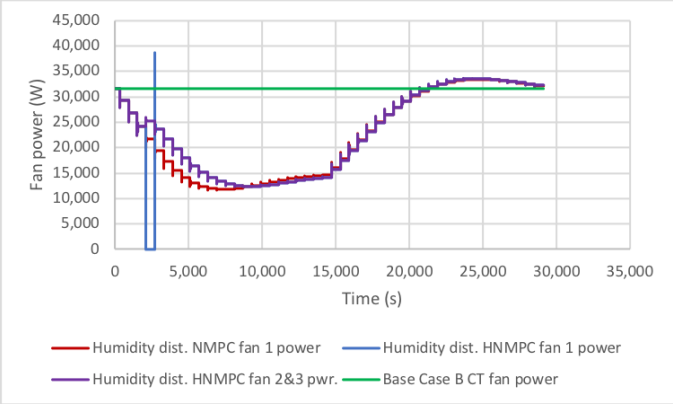

Figure 23: Cooling tower fan power during ambient humidity disturbance scenario.

this scenario, the NMPC and HNMPC controllers take the same action. The controllers are able to reduce the total power consumption and cost by 44.1% compared with Base Case A over the 24 hour simulation period (the electricity pricing is the same over the 24 hour period).

From Figure 10 and Figure 11 it can be seen that the controllers reduce the fan speeds by a greater degree than the pump speeds. The controllers find an optimal ratio between fan and pump speed for the cooling and temperature control requirement, given the power minimisation objective.

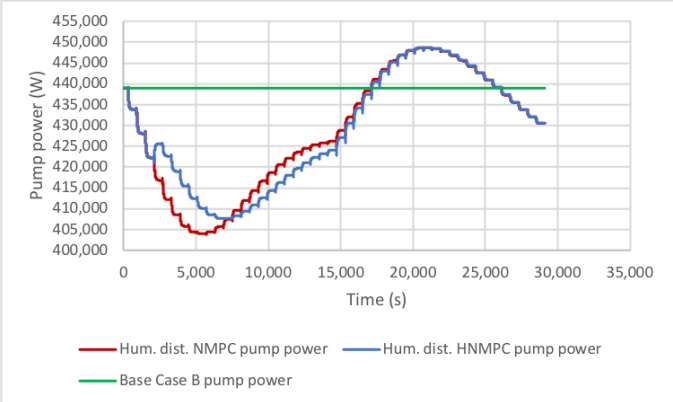

Figure 24: Cooling water pump power during ambient humidity disturbance scenario.

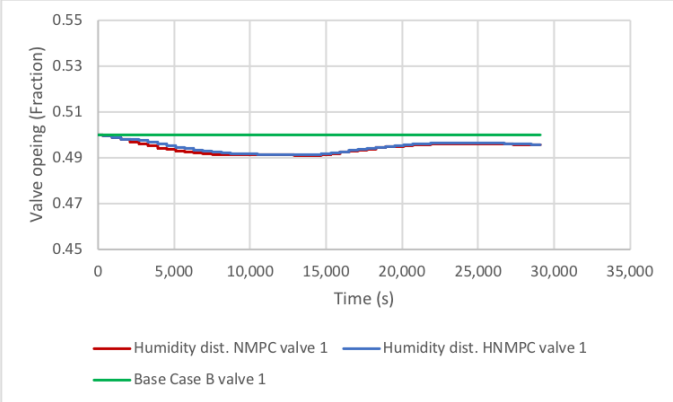

Figure 25: Cooling water valve 1 movement during ambient humidity disturbance scenario.

4.5.2. Base Case B

In Table 5 the Integral Square Error (ISE) sums and the total power consumption are shown for each scenario. The ISE is calculated as the difference between the normalised controlled variable (actual divided by engineering unit range) and the normalised set point, squared and totalled for the whole simulation period. The ISE figure tabled is the sum of the 11 temperature CV ISE figures.

Both the NMPC and HNMPC controllers succeeded in controlling the temperature well in the face of significant disturbances (see Figures 12, 17 and 22).

Table 4: Comparison of 24 hour power minimisation scenario.

Cntrl. strategy	**Power (kWh)**	**Cost (USD)**	**Power reduction vs. Base Case A**
Base Case A	52,826	2,536	0%
NMPC & HNMPC	29,543	1,418	44.1%

Table 5: Comparison of 8 hour disturbance rejection scenarios and control strategy runs.

Scenario & control strategy	**Temp. ISE**	**Temp. ISE reduction vs. NMPC**	**Power (kWh)**	**Power reduction vs. Base Case B**
Load dist., NMPC	3.10E-04	0%	4,051	48.5%
Load dist., HNMPC	2.58E-04	16.6%	4,255	45.9%
Amb. temp. dist., NMPC	1.06E-05	0%	7,289	7.3%
Amb. temp. dist., HNMPC	2.33E-06	78.0%	7,537	4.1%
Amb. hum. dist., NMPC	5.99E-06	0%	7,395	5.9%
Amb. hum. dist., HNMPC	5.56E-06	7.3%	7,410	5.7%
Base Case B power			7,860	0%

The HNMPC controller performed better than the NMPC controller, particularly when rejecting the ambient temperature disturbance for which its temperature ISE score was 78% smaller. The reduction in power consumption shown in Table 5 is due mainly to the controllers turning down the rotating equipment in order to control temperature. The power consumed by the NMPC and HNMPC controllers is less than that of Base Case B, with the biggest reduction occurring in the load disturbance scenario.

Since the objective function (9) is tuned to focus the controllers on temperature control (Table 3), the HNMPC controller uses the extra degrees of freedom it has compared to the continuous controller to further improve tem-

perature control as can be seen in the second and third columns of Table 5. This improved temperature control comes at the cost of slightly higher power consumption compared to the continuous controller (see last column of Table 5).

4.6. Monetary benefit

Monetary benefit estimation of advanced control and optimisation for the cooling water network is focused on electricity consumption minimisation in this paper. Advanced process temperature control also has significant monetary benefits, but quantification of those benefits is different for each sub-plant serviced by the different cooling water heat exchangers, and is beyond the scope of this paper. The estimated savings achieved by the NMPC/HNMPC control strategies is therefore derived from the power minimisation scenario and compared with Base Case A.

The NMPC and HNMPC controllers achieved a significant reduction in power consumption over Base Case A while maintaining the temperature at setpoint (Figure 9). These gains come from the reduction in fan and pump speeds as shown in Figures 10 and 11. The daily power cost savings is estimated to be USD 1,118 (2,536 - 1,418) as shown in Table 4. Assuming that the full design cooling capacity of the cooling water network is effectively not needed for 70% of the year and that these benefits can be achieved for that period of time, the annual total saving is USD 285,540.

The capital cost of making the cooling water network amenable to advanced control (Section 2.3) is estimated at USD 243,000. Assuming the implementation of HNMPC as per the design in this paper is done by the plant owner's control engineers, a cost of capital discount rate of 8%, and annual inflation of 2%, then the business case is a 10 year NPV of USD 1,829,251, an IRR of 120% and a 0.95 year payback period.

The electricity rates in the Arabian Gulf are typically lower than most other economies. The benefits of the control strategies developed in this paper could be increased in other markets because of potentially higher pricing of electricity.

In addition, if improved temperature control is taken into account as well, the benefits of advanced control will be even larger.

4.7. Computation platform

All simulations were conducted on a 2.5 GHz Intel Core i7 computer with 16 GB memory. The code was compiled in C++ 11 and ran on the Mac OS 10.13 operating system. This platform takes 33.1 seconds to run the plant model (Viljoen et al., 2018) in open-loop for 8 hours of simulation time. Running the HNMPC controller in closed-loop requires an average of 66.99 seconds per iteration, which is well within the 10-minute running interval indicated in Table 3. It takes 54.1 minutes for the closed-loop simulation to complete an 8-hour simulation time period. The NMPC gradient descent optimiser assists in limiting the time needed to execute the NMPC control algorithm, by not requiring the Hessian but only the Jacobian of the objective function to be calculated.

4.8. Conclusion

This paper showed how an NMPC and HNMPC controller can successfully control hydrocarbon temperatures, as well as minimise the power consumption of a cooling water network represented by a fundamental process model. The continuous MVs used by the NMPC controller can be combined with Boolean MVs in an HNMPC controller where the rotating equipment are switched on and off as needed.

The NMPC and HNMPC controllers are able to exploit the power minimisation opportunity whenever the cooling requirement and ambient conditions allow it by optimally decreasing fan and pump speeds from their original design settings while controlling temperature. This results in significant annual savings in electricity costs for the plant owner, as estimated in Section 4.6.

The HNMPC controller is able to perform well for a range of plant states and conditions. Large plant disturbances such as a reduction of the hydrocarbon mass flow to the cooling water exchangers, and large changes in ambient temperature and humidity conditions, can be controlled, contained and managed by the HNMPC control system.

The HNMPC controller performs better than the NMPC controller due to it having access to Boolean MVs and hybrid plant states in addition to the continuous MVs. This greater flexibility enables the HNMPC controller to better minimise the objective function and drive the plant towards an optimum state.

Overall hybrid NMPC has great potential for online optimisation of the cooling water networks of processing facilities. Normally plants of this kind do not have variable speed drives for the fans and pumps. This paper has shown that these MVs are effective in enabling NMPC to deal with typical conditions that occur on industrial cooling water networks. A capital investment roadmap could take a phased approach to first install variable speed drives and continuous NMPC, followed by a second phase of hybrid NMPC. Power consumption cost savings (Matthews and Craig, 2013; Muller and Craig, 2016) should be able to justify a business case for actuation and HNMPC control of such plants.

5. Acknowledgements

This work is based on research supported in part by the National Research Foundation of South Africa (Grant Number 111741).

References

Abbas, M. A., Milman, R., Eklund, J. M., 2017. Obstacle avoidance in real time with non-linear model predictive control of autonomous vehicles. Canadian Journal of Electrical and Computer Engineering 40, 12–22.

Al-Bassam, E., Alasseri, R., 2013. Measurable energy savings of installing variable frequency drives for cooling towers fans, compared to dual speed motors. Energy and Buildings 67, 261–266.

Allgower, F., Zheng, A., 2000. Nonlinear Model Predictive Control. Springer Basel, Basel, Switzerland.

Bakosova, M., Oravec, J., 2014. Robust model predictive control for heat exchanger network. Applied Thermal Engineering 73, 924–930.

Bartholomew-Biggs, M., 2000. Automatic differentiation of algorithms. Journal of Computational and Applied Mathematics 124, 171–190.

Bauer, M., Craig, I. K., 2008. Economic assessment of advanced process control a survey and framework. Journal of Process Control 18, 2–18.

Baydin, A. G., Pearlmutter, B. A., Radul, A. A., Siskind, J. M., 2018. Automatic differentiation in machine learning: A survey. Journal of Machine Learning Research 18, 1–43.

Belotti, P., Kirches, C., Leyffer, S., Linderoth, J., Luedtke, J., Mahajan, A., 2013. Mixed-integer nonlinear optimization. Acta Numerica 22, 1–131.

Biegler, L. T., Yanga, X., Fischer, G. A. G., 2015. Advances in sensitivity-based nonlinear model predictive control and dynamic real-time optimization. Energy 30, 104–116.

Boyd, S., Vandenberghe, L., 2004. Convex Optimization. Cambridge University Press, New York, USA.

Bryson, A. E., 1975. Applied optimal control - optimization, estimation, and control. Taylor and Francis Group, New York, USA.

Cacchiani, V., DoAmbrosio, C. C., 2016. A branch-and-bound based heuristic algorithm for convex multi-objective minlps. European Journal of Operational Research, 2–38.

Calamai, P. H., More, J. J., 1987. Projected gradient methods for linearly constrained problems. Mathematical Programming 39, 93–116.

Camacho, E. F., Bordons, C., 2007. Model Predictive Control, 2nd Edition. Springer-Verlag, London, UK.

Camacho, E. F., Ramirez, D. R., Limon, D., de la Pena, D. M., Alamo, T., 2010. Model predictive control techniques for hybrid systems. Annual Reviews in Control 34, 21–31.

Castro, M. M., Song, T. W., Pinto, J. M., 2000. Minimization of operational costs in cooling water systems. Transactions of the Institution of Chemical Engineers 78, 192–201.

Conceicao, A. S., Moreira, A. P., Costa, P. J., 2008. A nonlinear model predictive control strategy for trajectorytracking of a four-wheeled omnidirectional mobile robot. Optimal Control Applications and Methods 29, 335–252.

DeHaan, D., Guay, M., 2007. A real-time framework for model-predictive control of continuous-time nonlinear systems. IEEE transactions on automatic control 52 (11), 2047–2057.

Deng, K., Sun, Y., Li, S., Lu, Y., Brouwer, J., Mehta, P. G., Zhou, M., Chakraborty, A., 2015. Model predictive control of central chiller plant with thermal energy storage via dynamic programming and mixed-integer linear programming. IEEE Trans. on Automation Science and Engineering 12 (2), 565–579.

Dzedzemane, R., le Roux, J. D., Muller, C. J., Craig, I. K., 2018. Steam header state-space model development and validation. IFAC-PapersOnLine 51 (21), 207–212.

Findeisen, R., Allgower, F., Biegler, L. T., 2007. Assessment and Future Directions of Nonlinear Model Predictive Control. Springer-Verlag, Berlin, Germany.

Fletcher, R., 1987. Practical Methods of Optimization. John Wiley and Sons, West Sussex, England.

Floudas, C. A., 1995. Nonlinear and Mixed-Integer Optimization. Oxford University Press, New York, USA.

Ghadimi, E., Feyzmahdavian, H. R., Johansson, M., July 2015. Global convergence of the heavy-ball method for convex optimization. In: European Control Conference. IFAC, Linz, Austria, pp. 310–315.

Giftthaler, M., Neunert, M., Stäuble, M., Buchli, J., May 2018. The control toolbox an open-source C++ library for robotics, optimal and model predictive control. In: 2018 IEEE International Conference on Simulation, Modeling, and Programming for Autonomous Robots (SIMPAR). IEEE, Brisbane, QLD, Australia.

Giftthaler, M., Neunert, M., Stäuble, M., Frigerio, M., Semini, C., Buchli, J., 2017. Automatic differentiation of rigid body dynamics for optimal control and estimation. Advanced Robotics 31 (22), 1225–1237.

Goodfellow, I., Bengio, Y., Courville, A., 2016. Deep Learning, 1st Edition. The MIT Press, Massachusetts, USA.

Grüne, L., Pannek, J., 2017. Nonlinear Model Predictive Control Theory and Algorithms, second edition Edition. Oxford University Press, Springer, Switzerland.

Grüne, L., Pannek, J., Seehafer, M., Worthmann, K., December 2012. Analysis of unconstrained nonlinear mpc schemes with time varying control horizon. In: Proceedings of the 51st IEEE Conference on Decision and Control. IEEE, Maui, Hawaii, USA, pp. 2605–2610.

Guerreiro, B. J., Silvestre, C., Cunha, R., Pascoal, A., 2014. Trajectory tracking nonlinear model predictive control for autonomous surface craft. IEEE Transactions on Control Systems Technology 22 (6), 2160–2175.

Iusem, A. N., 2003. On the convergence properties of the projected gradient method for convex optimization. Computational and Applied Mathematics 22 (1), 37–52.

Li, X., Li, Y., Seem, J. E., Li, P., June 2012. Extremum seeking control of cooling tower for self-optimizing efficient operation of chilled water systems. In: Proceedings of the 2012 American Control Conference. IFAC, Montréal, Canada, pp. 2322–2330.

Long, C. E., Polisetty, P. K., Gatzke, E. P., 2007. Deterministic global optimization for nonlinear model predictive control of hybrid dynamic systems. International Journal of Robust and Nonlinear Control 17, 1232–1250.

Lucia, S., Finkler, T., Engell, S., 2013. Multi-stage nonlinear model predictive control applied to a semi-batch polymerization reactor under uncertainty. Journal of Process Control 23, 1306–1319.

Ma, Z., Wang, S., Xiao, F., 2008. Online performance evaluation of alternative control strategies for building cooling water systems prior to in situ implementation. Applied Energy 86, 712–721.

Marques, C. A. X., Fontes, C. H., Embiruu, M., Kalid, R. A., 2009. Efficiency control in a commercial counter flow wet cooling tower. Energy Conversion and Management 50, 2843–2855.

Matthews, B., Craig, I. K., 2013. Demand side management of a run-of-mine ore milling circuit. Control Engineering Practice 21 (6), 759–768.

Mayer, B., Killian, M., Kozek, M., 2016. A branch and bound approach for building cooling supply control with hybrid model predictive control. Energy and Buildings 128, 553–566.

Mayne, D. Q., 2014. Model predictive control: Recent developments and future promise. Automatica 50, 2967–2986.

Muller, C. J., Craig, I. K., 2015. Modelling of a dual circuit induced draft cooling water system for control and optimisation purposes. Journal of Process Control 25, 105–114.

Muller, C. J., Craig, I. K., 2016. Energy reduction for a dual circuit cooling water system using advanced regulatory control. Applied Energy 171, 287–295.

Muller, C. J., Craig, I. K., 2017. Economic hybrid non-linear model predictive control of a dual circuit induced draft cooling water system. Journal of Process Control 53, 37–45.

Muller, C. J., Craig, I. K., Ricker, N. L., 2011. Modelling, validation, and control of an industrial fuel gas blending system. Journal of Process Control 21 (6).

Negrete, R. L., D-Amato, F. J., 2013. Fast nonlinear model predictive control - formulation and industrial process applications. Computers and Chemical Engineering 51, 55–64.

Neidinger, R. D., 2010. Introduction to automatic differentiation and Matlab object-oriented programming. Society for Industrial and Applied Mathematics Review 52 (3), 545–563.

Nocedal, J., Wright, S. J., 2006. Numerical Optimization, second edition Edition. Springer, New York, USA.

Polyak, B. T., 1964. Some methods of speeding up the convergence of iteration methods. USSR Computational Mathematics and Mathematical Physics 4, 1–17.

Qian, N., 1999. On the momentum term in gradient descent learning algorithms. Neural Networks 12, 145–151.

Ricker, N. L., Muller, C. J., Craig, I. K., 2012. Fuel-gas blending benchmark for economic performance evaluation of advanced control and state estimation. Journal of Process Control 22 (6), 968–974.

Rubio-Castro, E., Serna-Gonzalez, M., Ponce-Ortega, J. M., El-Halwagi, M. M., 2013. Synthesis of cooling water systems with multiple cooling towers. Applied Thermal Engineering 50, 957–974.

Saidur, R., Mekhilef, S., Ali, M. B., Safari, A., Mohammed, H. A., 2012. Applications of variable speed drive (VSD) in electrical motors energy savings. Renewable and Sustainable Energy Reviews 16, 543–550.

Saudi Electricity Company, 2019. Saudi Arabia Electricity consumption tariffs. `https://www.se.com.sa/en-us/customers/Pages/TariffRates.aspx`, accessed: 2019-01-31.

Sridhar, U. M., Govindarajan, A., Rhinehar, R. R., 2016. Demonstration of leapfrogging for implementing nonlinear model predictive control on a heat exchanger. ISA Transactions 60, 218–227.

Stroustrup, B., 2013. The C++ Programming Language, 4th Edition. Pearson Education Inc., Upper Saddle River, NJ, USA.

Sutskever, I., Martens, J., Dahl, G., Hinton, G., June 2013. On the importance of initialization and momentum in deep learning. In: Proceedings of the 30 th International Conference on Machine Learning. ICML, Atlanta, USA, pp. 1139–1147.

Viljoen, J. H., Muller, C. J., Craig, I. K., 2018. Dynamic modelling of induced draft cooling towers with parallel heat exchangers, pumps and cooling water network. Journal of Process Control 68, 34–51.

Walther, A., 2007. Automatic differentiation of explicit Runge-Kutta methods for optimal control. Computational Optimization and Applications 36 (1), 83–108.

Wang, L., 2009. Model Predictive Control System Design and Implementation Using MATLAB, 1st Edition. Springer-Verlag, London, UK.

Wright, M. H., 2004. The interior-point revolution in optimization: History. Recent Developments, and Lasting Consequences, American Mathematical Society 42 (2).

Yin, X. H., Li, S., 2018. Energy efficient predictive control for vapor compression refrigeration cycle systems. IEEE/CAA Journal of Automatica Sinica 5 (5).